

Optimal sizing and allocation of energy storage in wind power incorporated optimal power flow

Ulagammai Meyyappan* and Kumudini Devi Raguru Pandu**

The rapid expansion of wind power creates new challenges for power system operators and electricity marketers. Wind energy has the potential benefits in curbing emissions and reducing the consumption of irreplaceable reserves. But the variable nature of wind energy poses challenges in the power system operation and planning. In order to ensure the wind power as firm power, energy storage is added to smoothen the variations in wind power. In this paper, optimal power flow with wind and energy storage is developed. The Energy Storage Systems (ESS) are installed as a backup of wind generators to meet the demand reliably. The objective is to minimize the loss by optimal location and sizing of ESSs. With the optimally located ESSs, OPF is carried out using SFLA and tested on IEEE 30 bus system.

Keywords: *Wavelet neural network, shuffled frog leap algorithm, optimal power flow, energy storage systems*

Nomenclature :

η_{ch}	-	Charging efficiency of the energy storage system
a_i, b_i and c_i	-	Cost coefficients of the i^{th} thermal unit
$F_i(P_i)$	-	Cost function of the i^{th} thermal unit in INR/hr
$F_j(W_j)$	-	Cost function of the j^{th} wind generation unit in INR/hr,
v_i	-	cut-in wind speed(m/s); v_r - rated wind speed(m/s); v_o - cut-out wind speed (m/s).
d_j	-	Direct cost of the j^{th} wind generator unit
η_{dis}	-	Discharge efficiency of the energy storage system
$E_{storagei,t+1}$	-	Energy storage at t+1 hour
k_p, k_r	-	Penalty cost and Reserve cost (INR/MW)

$f_w(W)$	-	Probability Density Function of the wind power as Weibull distribution
$f_v(v)$	-	Probability Density Function of the wind speed as Weibull distribution
W_r	-	Rated power (MW) ; $W_{i,av}$ Available wind power (MW) ;
c	-	Scale factor in Weibull distribution
k	-	Shape factor in Weibull distribution
W	-	Sheduled wind power (MW)
$SOC_{j,t+1}$	-	State of charge of jth device at t+1 hour
P_i	-	Thermal power generation of the i^{th} thermal unit in MW
NE	-	Number of Energy storage units

*Assistant Professor, EEE Department, Saveetha Engineering College Thandalam, Chennai - 602105, Tamil Nadu, India.

**Professor, College of Engineering - Guindy, Anna University, Chennai - 600025, Tamil Nadu, India.

NG	-	Total number of thermal units; M Total number of wind generating units
F_T	-	Total production cost (INR/hr),
W_j	-	Wind power generation of the j^{th} wind unit in MW

1.0 INTRODUCTION

Optimal Power Flow (OPF) aims to optimize a certain objective, subject to the network power flow equations and system and equipment operating limits. The optimal condition is attained by adjusting the available controls to minimize an objective function subject to specified operating and security requirements. Objective function takes various forms such as fuel cost, transmission losses and reactive source allocation. Usually the objective function of interest is the minimization of total production cost of scheduled generating units. This is mostly used as it reflects current economic dispatch practice and importantly cost related aspect is always ranked high among operational requirements in power systems.

Wind energy is estimated to account for a big share of renewable energy source but wind is variable and wind energy capacity does not directly turn into wind power generation. In order to increase the renewable energy penetration into the grid, utilities need to have costly reserve capacity online. As an alternative of this central reserve, many researchers have proposed energy storage solutions that can be allied with the renewable source. Energy storage significantly increases the use of the renewable source and makes this energy dispatchable as needed, resulting in a remarkable increase in the renewable energy value proposition. At present there are several types of energy storage technologies, which afford different characteristics, e.g. energy and power density, efficiency, cost, lifetime, and response time. Examples of energy storage systems are ultra capacitors, Superconducting Magnetic Energy Storage Systems (SMES), flywheel, batteries, compressed air, pumped hydro, fuel cells and flow batteries.

In terms of joint scheduling model for wind power and energy storage system, Xiongwu *et al* [1] in their paper considered the power generation units and energy storage units constraints and built a static model for wind power and energy storage joint operation. The uncertainty of wind power is ignored. Hu Zechem *et al* [2] combined the opportunity constraint theory and built a joint scheduling model of wind power and ESS considering wind power uncertainty. Huajie Diang *et al* [3] developed a wind storage joint scheduling model considering risk constraints and used Monte carlo simulation method.

In terms of solution technique, many methods have been proposed in the literature to solve power flow problem. The OPF problem is solved by several classical techniques like primal dual interior point [4], dynamic programming [5], linear programming and non-linear programming. These algorithms are applicable for continuous differentiable functions and not for non-smooth cost functions. The past decade has seen the introduction of other methods based on Artificial Intelligence (AI) techniques including GA, PSO, DE and hybrid DE [6] which have also been proposed to solve the OPF problem. This paper presents an evolutionary technique named shuffled frog leap algorithm (SFLA) which combines the benefits of the genetic based mimetic algorithms and the social behavior based PSO algorithms for solving OPF with wind and energy storage systems (ESS).

This paper is organized as follows: Wind speed forecasting and characterization are given in section 2.0. OPF problem formulation including wind generators and energy storage systems is presented in section 3.0. Section 4.0 describes the SFLA solution technique. Section 5.0 presents the simulation results for IEEE 30 bus system. Section 6.0 concludes the paper.

2.0 WIND SPEED FORECASTING AND CHARACTERIZATION

In last few decades, several methods for wind speed forecasting such as the ANN, PNN and the General Regressive Neural Networks (GRNN)

have been proposed. In general, ANNs are trained in a supervised fashion with the Back Propagation (BP) algorithm. The basic BP algorithm is a gradient descent one [7], which adjusts the network weights along the steepest descent direction of the error function. Other forecasting techniques PNN and GRNN explained in [8] are also considered for comparison and analysis.

All these methods suffer from obtaining monolithic global models for a time-series [9]. To enhance the ANNs ability in learning the signals, the hidden patterns (i.e) of all the frequency components from the data should be extracted. Hence to do this a multi-resolution decomposition technique such as wavelet transform is introduced.

Wavelet transform is a scalable windowing technique. It breaks the signals into shifted scaled versions of the original wavelet signal. It uses time scale region instead of time frequency region. In order to improve the accuracy of ANNs, they are combined with wavelet to set hybrid model [10]. The wind speed is first decomposed into several sub-serials using wavelet. To forecast each sub-serial, each neural network is constructed. The final wind speed forecasting result can be obtained by summing up all the sub-serial forecasting results. A given signal $s(t)$ is decomposed into several other signals with different levels of resolution by Dyadic Wavelet Transform (DWT), and the DWT of $s(t)$ is defined as follows:

$$s(m, n) = 2^{\frac{m}{2}} \int s(t) \varphi^* \left(\frac{t-n2^m}{2^m} \right) dt \quad \dots(1)$$

where the * denotes a complex conjugate, m and n are scale and time-shift parameters, respectively, and $s(t)$ is a given basis function (mother wavelet). The DWT is implemented using a multi-resolution pyramidal decomposition technique.

The WNN forecasting procedure shown in Figure 1 comprises a development of a preliminary forecast model followed by pre-signal processing, signal prediction and post-signal processing [10].

2.1 Stage 1: Pre-signal Processing

In pre-signal processing, historical wind speed data are fed to proposed model as time-series signals. The Non-decimated Wavelet Transform (NWT) is used as the pre-signal processor and depending on the selected resolution level, the respective time-series signals are decomposed into a number of wavelet coefficients. These decomposed coefficients are then normalized and fed as inputs to the signal predictor (Neural Networks) for either training or forecasting.

2.2 Stage 2: Signal Prediction

ANNs are used for signal prediction in the forecast model. The number of ANNs needed for the model is determined by the number of wavelet coefficient signals at the output of the pre-processor. For each wavelet coefficient signal (including the approximation component), one ANN is required to perform the corresponding prediction.

2.3 Stage 3: Post- Signal Processing

In post-signal processing, the same wavelet technique and resolution level as mentioned in pre-signal processing are used. In this stage, the outputs from the signal predictor (ANNs) are combined to form the final predicted output. This is achieved by summing all the predicted wavelet coefficients.

The wind speed profile at a given location closely follows Weibull distribution. The Weibull distribution function with a shape factor of 2 is also known as the Rayleigh distribution. In [11], the advantages of the Weibull distribution are noted as follows: 1) it is a two parameter distribution, which is more general than the single parameter Rayleigh distribution, but less complicated than the five-parameter bi-variate normal distribution; 2) it is already proven that the observed data of wind speeds follows a Weibull distribution; and 3) if the k and c parameters are known at one height, a methodology exists to find the corresponding parameters at another height.

The probability density function for a Weibull distribution is given by,

$$f_v(v) = \left(\frac{k}{c}\right)\left(\frac{v}{c}\right)^{k-1}e^{-\left(\frac{v}{c}\right)^k} \quad \dots(2)$$

Once the uncertain nature of the wind is characterized as a random variable, the output power of the Wind Energy Conversion Systems (WECS) may also be characterized as a random variable through a transformation from wind speed to output power. Ignoring minor nonlinearities, the output of the WECS with a given wind speed input may be stated as [12],

$$W = 0 \text{ for } v < v_i \text{ and } v > v_o \quad \dots(3)$$

$$W = W_r \frac{(v-v_i)}{(v_r-v_i)} \text{ for } v_i \leq v \leq v_r \quad \dots(4)$$

$$W = W_r \text{ for } v_r \leq v \leq v_o \quad \dots(5)$$

The wind speed has the Weibull distribution and it has to be converted as wind power distribution. This is achieved by linear transformation given below [13]:

$$W = T(V) = aV + b \quad \dots(6)$$

Where T is the transformation, W is wind power random variable, V is wind speed random variable. After the transformation the Weibull Probability Density Function (PDF) of wind power output random variable in continuous range takes the following form [12]

$$f_w(w) = \left(\frac{klv}{c}\right)\left(\frac{(1+\rho l)v_i}{c}\right)^{k-1}e^{-\left(\frac{(1+\rho l)v_i}{c}\right)^k} \quad \dots(7)$$

Then the area under the power distribution curve is calculated using trapezoidal rule and the discrete values of wind power are obtained as in author's previous paper [14].

3.0 OPF PROBLEM FORMULATION WITH WIND AND ENERGY STORAGE

Need for Energy storage: In order to effectively reduce CO₂ emissions, fossil fuel will be gradually replaced by renewable source to produce electrical power. Wind and solar are the most abundant renewable sources for electric power generation. Energy converted from wind and solar becomes more and more competitive in power markets due to the improvement of technology. However, the variable nature of renewable energy limits its large-scale penetration in the power system. Additional spinning reserves are always assigned with renewable generators committed to the system to ensure system reliability. The extra cost and emission of reserve units becomes another economic and environmental issue. However, energy storage could be a solution to these issues. Akhavan Hejazi and Mohsenian Rad [15] provided reliability evaluations for energy storage along with large-scale wind generation, and observed some potential benefits for both the power system operator and wind farm owners.

Energy storage for power systems has recently attracted significant interest and attention from researchers and the power industry. An energy storage system is treated as a generator (i.e. pumped hydro or stationary batteries) with a negative or positive output during its charging or discharging period, respectively. With fast response time and low operating cost, energy storage is viewed as an attractive resource to compensate the variable nature in the wind penetrated power system and as an essential resource to enable integration of large amounts of renewable resources into the electric grid. Examples of energy storage systems are ultracapacitors, Superconducting Magnetic Energy Storage systems (SMES), flywheel, batteries, compressed air, pumped hydro, fuel cells and flow batteries.

3.1 Problem Formulation

The objective of multiperiod (dynamic) OPF is to minimize the cost of generation and optimally utilize the renewable generation.

The objective function is given by,

$$\begin{aligned} \text{Min } F_T = & \sum_{t=1}^{24} \left(\sum_{i=1}^{NG} a_i P_{gi,t}^2 + b_i P_{gi,t} + c_i + \right. \\ & \left. \sum_{j=1}^M C_{opw} W_{j,t} + \sum_{k=1}^{NE} C_{ops} E_{storage\ k,t} \right) \end{aligned} \quad \dots(8)$$

Subject to the equality and inequality constraints

$$\sum_{i=1}^{24} \left(P_{G_{i,t}} - P_{D_{i,t}} - V_{i,t} \sum_{j=1}^N V_{j,t} [G_{ij} \cos(\delta_{i,t} - \delta_{j,t}) + B_{ij} \sin(\delta_{i,t} - \delta_{j,t})] = 0 \right) \quad \dots(9)$$

$$\begin{aligned} \sum_{t=1}^{24} \left(Q_{G_{i,t}} - Q_{D_{i,t}} - \right. \\ \left. V_{i,t} \sum_{j=1}^N V_{j,t} [G_{ij} \sin(\delta_{i,t} - \delta_{j,t}) + \right. \\ \left. B_{ij} \cos(\delta_{i,t} - \delta_{j,t}) \right] = 0 \end{aligned} \quad \dots(10)$$

Where $P_{G_{i,t}}$ & $Q_{G_{i,t}}$ are sum of the real power and reactive power injections (thermal, wind and energy storage) at bus i at time t .

$$P_{gi\ min} \leq P_{gi,t} \leq P_{gi\ max} \quad i = 1,2 \dots NG \quad \dots(11)$$

$$V_{gi\ min} \leq V_{gi,t} \leq V_{gi\ max} \quad i = 1,2 \dots NG \quad \dots(12)$$

$$Q_{gi\ min} \leq Q_{gi,t} \leq Q_{gi\ max} \quad i = 1,2 \quad \dots(13)$$

$$W_{j\ min} \leq W_{j,t} \leq W_{j\ max} \quad j = 1,2 \dots M \quad \dots(14)$$

$$E_{storage,kmin} \leq E_{storage\ k,t} \leq E_{storage\ k\ max} \quad k = 1,2 \dots NE \quad \dots(15)$$

$$S_{i,t} \leq S_{i\ max} \quad i = 1,2 \dots \text{No. of lines} \quad \dots(16)$$

Further state of charge of energy storage for a hour $t+1$ is given as,

$$\begin{aligned} E_{storage\ i,t+1} = SOC_{i,t+1} = \\ \begin{cases} SOC_{i,t} + \eta_{dis} P_K^{St} & \text{if } P_K^{St} < 0 \\ SOC_{i,t} + \eta_{ch} P_K^{St} & \text{if } P_K^{St} > 0 \end{cases} \end{aligned} \quad \dots(17)$$

where P_K^{St} is the power required from the k^{th} energy storage system at time t . It may take positive or negative value depending on the availability of

the wind power. If the availability of the wind power is less than the expected, then the energy storage starts discharging to meet the wind deficit and hence P_K^{St} takes negative value and vice-versa.

In short time scales it is not possible for a conventional generator to considerably deviate from current operating point. Therefore, we limit the amount of change in generation depending on the ramp rate of individual generators. The constraints are given as:

(a) When generation increases

$$P_{gi,t} - P_{gi,(t-1)} \leq UR_i \quad \dots(18)$$

(b) When generation decreases

$$P_{gi,(t-1)} - P_{gi,t} \leq DR_i \quad \dots(19)$$

For $i = 1,2, \dots, NG$

where UR_i and DR_i are the ramp-up and ramp-down limits of i^{th} unit in MW.

Optimal location and sizing of ESS

The determination of optimal location and size of ESS is posed as an optimization problem.

The problem can be stated as :

To find the optimal location and size of ESS by minimizing transmission losses while satisfying equality and inequality constraints.

$$\text{Min } x \quad P_{loss} \quad \dots(20)$$

Where $x = [P_{g2} \dots P_{gNG}, W_1 \dots W_M, E_{storage\ 1} \dots E_{storage\ NE}]$

Subject to constraints (11) to (17)

The optimization problem is executed for different wind power penetrations. The location and size of ESS is the super set of all the optimal solutions.

Optimal power flow analysis considering the entire wind power distribution is carried out using fmincon and SFLA technique.

4.0 SHUFFLED FROG LEAP ALGORITHM SOLUTION TECHNIQUE

It is a memetic algorithm inspired by the food hunting behavior of frogs. It is based on the evolution of memes carried by the interactive frogs and by the global exchange of information among themselves. It is a combination of deterministic and random approaches. It also combines the benefits of both the genetic based memetic algorithm and social behavior based PSO algorithm. It can be used to solve many complex optimization models that are non linear and non differentiable.

The first step of this algorithm is to generate initial population P of frogs randomly in search space. The position of i^{th} frog is represented as, $X_i = [X_{i,1}, \dots, X_{i,D}]$ where D is the number of variables. Then the frogs are sorted in descending order according to their fitness. After that, the entire population is partitioned into m subsets referred as memeplexes each containing n frogs ($P = m * n$). The strategy of the partitioning is as follows: The first frog goes in to first memeplex, second goes to second memeplex, the m^{th} frog to m^{th} memeplex and $(m+1)$ frog goes to first memeplex and so forth. In each memeplex the position of frogs with the best and worst are identified as X_b and X_w respectively. Also the position of the frog with global best is X_g . Then within each memeplex a process similar to PSO algorithm is applied to improve only the frog with worst fitness in each cycle using the following equation:

Change in frog position is given by,

$$D_i = rand() * (X_b - X_w) \dots(21)$$

New position

$$X_w = \text{Current position of } X_w + D_i \text{ where } D_{imax} \geq D_i \geq -D_{imax} \dots(22)$$

Where $rand()$ is the random number between 0 and 1 and D_{imax} is the maximum allowed change in a frogs position.

Fitness function to be evaluated is given

$$\text{by, } F_T + \lambda (P_d \sim \sum_{i=1}^{N+M} P_i) \dots(23)$$

Figure 1 illustrates the memeplex partitioning process and Figure 2 shows the flowchart for SFLA

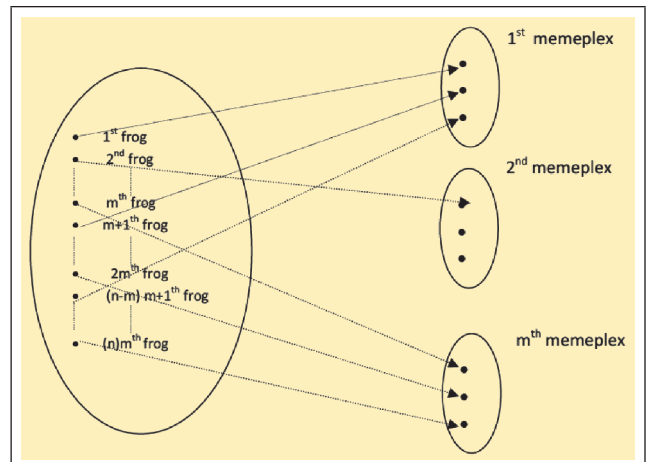


FIG. 1 MEMEPLEX PARTITIONING PROCESS

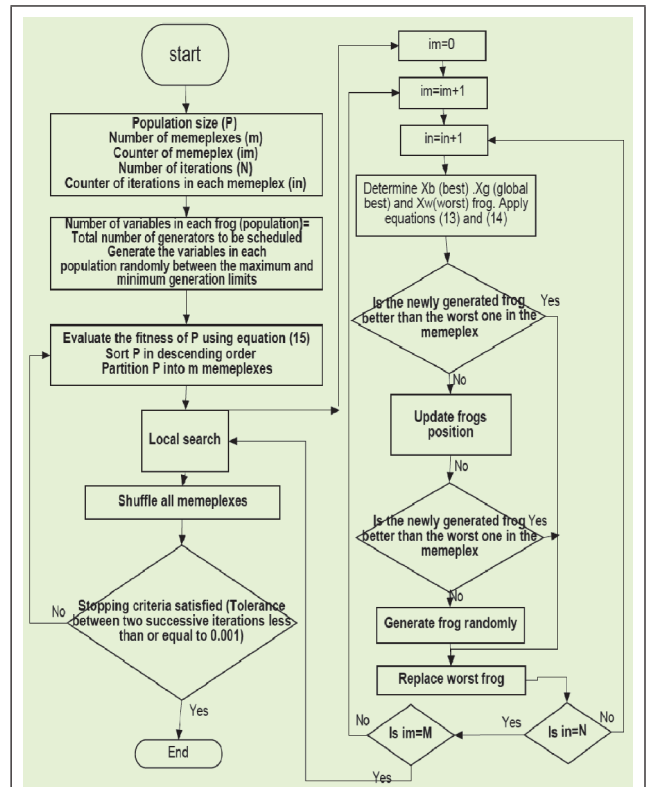


FIG. 2 SFLA FLOWCHART

5.0 RESULTS AND DISCUSSIONS

5.1 Wind Speed Prediction

The training data set and test data set comprise temperature, humidity, dew point, pressure, wind direction and wind speed. To evaluate the model proposed for wind speed prediction, data sets are collected from the automatic weather station and the study is conducted for 24 hours ahead. The sampled time series used in the model includes 1000 data in total, corresponding to 30 minutes of mean data. The time series is distinguished into two folders; one is the training set containing 964 samples used for the model’s training and the other is the test set that includes the rest, namely, 36 samples, used to verify the accuracy during the prediction period. Some of the data in [3] are deliberately multiplied by a constant (*10, *100 or *1000) to avoid storage of the floating point numbers and the same data is considered.

Different AI techniques such as FFBP, CFBP, PNN, GRNN and KNN are applied to the model developed in the author’s previous paper [10]. In WNN, the number of ANN required depends upon the wavelet family and the resolution level. With a resolution level of 2, the wavelet family is chosen as Db_2 . Hence, three neural networks are constructed for WNN. The individual ANN is constructed depending on the wavelet coefficients. In general, db_2 wavelet family produces four filter coefficients for single decomposition. By linear convolution, number of approximations (A) and detail coefficients (D) are given by $(m+n-1)/2$ where m is the input data size (number of inputs in this case is 15) and n is the filter coefficient size.

In this case, the number of A and D in the first level decomposition are,

$$\text{e.g: } A = D = (15+4-1)/2 = 9 .$$

For second level decomposition, the numbers of coefficients are: $(9+4-1)/2 = 6$.

Thus, the input neurons are 6, 6, and 9 for ANN₁, ANN₂, and ANN₃, respectively. Ten hidden

neurons and one output neuron (wind speed) is selected for all neural networks [6].

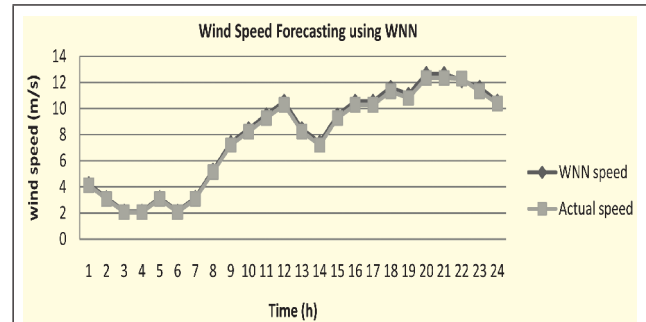


FIG. 3

The resultant relationships between the predicted and the actual values of the wind speed for the different ANN techniques are presented in [3]. Figure 3 displays the wind speed predicted by WNN. Performance measures such as Mean Square Error (MSE), Mean Absolute Percentage Error (MAPE) and linear regression are used to compare the various methods that are applied for wind speed predictions. These measures can be calculated using the equations in (3) and the comparison results are given in Table 1.

TABLE I COMPARISON OF PERFORMANCE MEASURES FOR DIFFERENT ANN TECHNIQUES						
	FFBP	CFBP	PNN	GRNN	KNN	WNN
MSE	6.74	6.81	3.795	2.85	5.88	2.7
MAPE (%)	5.10	5.26	2.972	2.3002	0.91	1.55

According to the forecasted errors WNN has the lowest MSE and MAPE; hence, the WNN model is used for wind speed prediction. GRNN is ranked second followed by PNN and KNN, respectively. Thus WNN is found to be the better wind speed-predicting technique compared with the other ANN techniques. The shape factor and scale factor of Weibull distribution for the predicted wind speed is obtained as 2.24 and 8.83 respectively. The cut-in speed, cut-out speed and rated speed in the Weibull distribution are considered as 2, 10 and 15 m/s respectively. The wind power is predicted for every hour by using the equation (3).

5.2 OPF Results

Simulations are carried out using IEEE 30 bus system using SFLA technique. The standard IEEE 30 bus system has 6 generators and 22 load buses. A wind generator of capacity 260 MW is integrated at bus 7 which has high short circuit level. In SFLA, the control parameters are power generated by the thermal and wind units. Hence, the number of control variables for this test system is 7 (6 thermal + 1 wind generator). The population size for SFLA is assumed to be 50 with 5 memplexes. The maximum number of iterations is 100. Results of OPF with wind using SFLA are presented in Table 2.

TABLE 2	
OPF RESULTS OF IEEE 30 BUS SYSTEM WITH WIND GENERATOR (P _D -283.4 MW)	
Control variables	SFLA
P ₁ (MW)	26.12
P ₂ (MW)	21.72
P ₅ (MW)	14.58
P ₈ (MW)	16.13
P ₁₁ (MW)	17.54
P ₁₃ (MW)	30.82
P ₇ (MW)	166.09
V ₁ (pu)	1.06
V ₂ (pu)	1.04
V ₅ (pu)	1.00
V ₈ (pu)	1.01
V ₁₁ (pu)	1.01
V ₁₃ (pu)	1.05
V ₇ (pu)	1.05
Cost (INR/hr)	784.23
Losses (MW)	9.36
Exe.Time (Sec)	124

The computational time for SFLA the time is around 124 seconds for 100 trials. It can be seen from the table that the operation cost gets reduced with the inclusion of wind power. The operational cost and loss without wind generator using PSO is 800.41 INR/hr and 12.96 MW respectively (Abido 2002). But with the inclusion of wind power the operational cost gets reduced from 800.41 INR/hr to 794.57 INR/hr. Also the

transmission losses get reduced from 12.96 MW to 9.36 MW.

5.3 OPF with wind and Energy storage

This section presents about the determination of optimal location and sizing of ESS with loss minimization as objective. For this case different wind power penetrations are considered. Hence discrete values of wind power are considered. Three distinct values of wind power allowing 10% of forecast errors are considered for OPF (i) Forecasted wind power (wp) (ii) wp+(0.1*wp) and (iii) wp-(0.1*wp) are taken and presented in Table 3 and shown in Figure 4. Along with these wind power values, two extreme cases nil wind and rated wind power are also considered for allocation of ESSs. Initially, SFLA initializes a random ESS size for each bus and the size at each bus will be updated by SFLA. At the end, the size of ESSs at some buses becomes zero, which means that these buses do not need to install any ESS. The remaining ESSs converge to their optimal allocations. The total operation cost and power loss is reduced, and voltage profiles are improved and the results are presented in Table 4. The objective function considered here is the minimization of the losses. The installation of ESS's at proper locations may reduce the transmission losses.

TABLE 3					
DISCRETIZATION OF WIND POWER					
Wind power (MW)	0	69.3	77.03 (mean)	84.06	260 (rated)
Probability	7.12	23.67	38.39	21.9	8.92

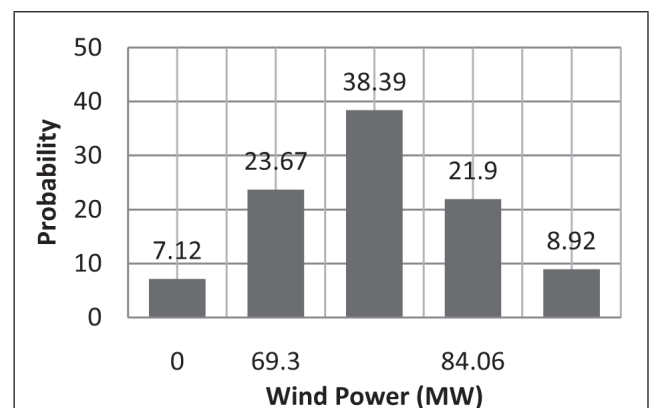


FIG. 4 DISCRETIZATION OF WIND POWER

TABLE 4					
OPF WITH ESS CONSIDERING DISCRETIZED WIND POWER					
Bus No.	Deterministic OPF				
	Wind Power (MW)				
	0	69.3	77.03 (mean)	84.06	260 (rated)
	PG(MW)	PG(MW)	PG(MW)	PG(MW)	PG(MW)
1	96.63	99.38	86.432	83.123	8.23
2	0	17.12	77.03	157.09	260
3	13.8983	18.4	0	0	0
4	0	0	0	0	0
5	6.7939	8.88	5.73	7.12	3.37
6	0	3.67	1.73	2.62	0
7	10.911	8.76	7.138	6.073	0
8	9.4697	12.46	10.34	11.39	0
9	0	0	0	0	0
10	0	0	0	0	0
11	17.67	13.67	11.681	10.734	2.13
12	0	0	0	0	0
13	32.98	29.67	31.68	25.43	0
14	0	0	0	0	0
15	5.54	0	0	0	0
16	10.87	5.5	0	0	0
17	0	0	0	0	0
18	0	0	0	0	0
19	11.795	10.86	13.738	5.67	2.156
20	13.059	12.156	14.368	7.156	1.95
21	0	0	0	0	0
22	14.7986	15.87	16.13	6.8	3.67
23	0	0	0	0	0
24	5.9658	6.86	4.794	1.12	4.37
25	14.317	11.32	12.034	7.32	0
26	0	0	0	0	0
27	11.7016	13.70	11.070	0	0
28	0	0	0	0	0
29	8.18	7.17	5.17	4.2	5.12
30	7.37	6.17	7.18	1.3	0
Losses (MW)	8.7901	8.64	8.412	8.23	7.98

From the results, it is obvious that injection of power at the buses 11, 19, 20, 22, 24 and 29 (the highlighted bus locations in Table 3 is needed to reduce the losses. Hence these buses are considered as the optimal location for installing ESSs. From the values of generations obtained,

the capacity of each ESS can be fixed as 20 MW each. For optimal allocation of generation and for the minimization of the loss, 6 ESSs are installed with a total capacity of 120 MW.

From the above results, the ESS locations are identified as 11, 19,20,22,24 and 29 with a maximum rating of 20 MW each. Optimal power flow is run considering entire wind power distribution and the results are presented in Table 5 for IEEE 30 bus system.

TABLE 5	
OPF WITH WIND AND OPTIMALLY LOCATED ESS	
IEEE 30 bus (Pd -283.4)	
Control & dependent variables	SFLA
P ₁ (MW)	32.51
P ₂ (MW)	14.09
P ₅ (MW)	29.82
P ₈ (MW)	28.45
P ₁₁ (MW)	39.14
P ₁₃ (MW)	18.376
Sum of 6 ESSs (MW)	83.8
Wind -P ₇ (MW)	45.2
V ₁ (pu)	1.060
V ₂ (pu)	1.02
V ₅ (pu)	1.030
V ₈ (pu)	1.01
V ₁₁ (pu)	1.00
V ₁₃ (pu)	1.010
V ₇ (pu)	0.998
Average V (pu) of all ESSs	1.102
Cost(INR/Hr)	775.21
Losses (MW)	8.56
Exe Time (sec)	(100 trials)

The above obtained results with and without ESS are compared and given in Table 6. From the comparison analysis, with the installation of ESS, the cost obtained is slightly less than the cost without ESS. The bus voltages for all the cases are within their limits. Losses obtained with optimal location of ESS are 9.98 MW and 8.56

MW respectively by PDIP and SFLA. Around 2% of the loss reduction can be achieved with the help of optimally located ESSs.

TABLE 6		
COMPARISON OF OPF WITH AND WITHOUT ESS		
Case Study	Cost (INR/hr)	Loss (MW)
OPF without ESS	784.23	9.36
OPF with optimally located ESS	775.21	8.56

6.0 CONCLUSION

As wind penetration continues to increase in the power grids, it becomes important to consider the uncertainty of wind power when optimizing the placement and size of energy storage systems. In this paper, SFLA algorithm is proposed to determine the optimal ESS allocation in wind penetrated power systems. Unlike many other optimization methods which only consider the worst case (zero wind) scenario, the entire wind power distribution is considered here. A five-point estimation method is implemented to discretize the continuous wind power distribution. IEEE 30-bus and 118 bus system are considered as case studies. The results show that the proposed SFLA is able to find proper location and size of ESS as well as minimizes the total operation cost and losses and also improves the voltage profile.

REFERENCES

- [1] X Wu, X Wang, J Li, A joint operation model and solution for hybrid wind energy storage systems Proc CSEE Vol. 33, pp. 10–7, 2013.
- [2] H Zechun, D Huajie, K Tao, A joint daily operational model for wind power and pumped-storage plant Automat Electric Power Syst Vol. 36, No. 2, pp. 36-41, 2012.
- [3] H Ding, Zechun Hu, Yonghua Song. Stochastic optimization of the daily operation of wind farm and pumped-hydro-storage plant Renewable Energy, Vol. 48, 2012.
- [4] F Capitanescu, M Glavic, Damien Ernest and Louis Wehenkel Interior point based algorithms for the solution of optimal power flow problems — Electric Power System Research, Vol. 77, pp. 507-518, June 2006
- [5] S Granville, J C Mello, and A C G Melo, Application of Interior Point method to Power flow Unsolvability, IEEE Transactions on Power Systems, Vol. 11, No. 2, pp. 1096-1103, May 1996
- [6] A Bhattacharya, and Pranab Kumar Chattopadhyay, Discussion of A Hybrid Interior Point Assisted Differential Evolution Algorithm for Economic Dispatch, IEEE Transactions On Power Systems, Vol. 27, No. 2, pp. 1142, May 2012.
- [7] W Y Chang, Application of Back Propagation Neural Network for Wind Power Generation Forecasting International Journal of Digital Content Technology and its Application, 7, 502-509, 2013.
- [8] D F Specht, A General Regression Neural Network, IEEE Transactions on Neural Networks, Vol. 2, No. 6, pp. 568–576, November 1991.
- [9] J Shi, J Guo and S Zheng, Evaluation of hybrid forecasting approaches for wind speed and power generation time series Journal of Renewable and Sustainable Energy Reviews, 16, pp. 3471-3480, 2012.
- [10] S Dhivya, M Ulagammai & Kumudini Devi, R P, Performance Evaluation Of Different Ann Models for Medium Term Wind Speed Forecasting, International journal of Wind Engineering, Vol. 35, No. 4, pp. 433-444, 2011.
- [11] E K Akpınar and S Akpınar, Statistical analysis of wind energy potential on the basis of the Weibull and Rayleigh distributions for Agin-Elazığ, Turkey. Journal of Power and Energy, 218: pp. 557-565, 2004.

- [12] A N Celik, A statistical analysis of wind power density based on the Weibull and Rayleigh models at the southern region of Turkey. *Renewable Energy*, Vol. 29, No. 4, pp. 593-604, 2004.
- [13] J Hetzer, Y, C David and Kalu Bhattarai, An Economic Dispatch Model Incorporating Wind Power, *IEEE Transactions On Energy Conversion*, Vol. 23, No. 2, pp. 603-612, 2008.
- [14] J A Carta, P Ramirez and S Velázquez, A review of wind speed probability distributions used in wind energy analysis: Case studies in the canary islands, *Renewable Sustainable Energy Rev.*, Vol. 13, No. 5, pp. 933-955, 2009.
- [15] U Meyyappan and K D R Pandu, Wavelet Neural Network-based Wind-power Forecasting in Economic Dispatch: A Differential Evolution, Bacterial Foraging Technology, and Primal Dual-interior Point Approach, *Electric Power Components and Systems*, Vol. 43, No. 13, pp. 1–12, 2015.
- [16] H Akhavan-Hejazi, H Mohsenian-Rad, Optimal operation of independent storage systems in energy and reserve markets with high wind penetration, *IEEE Transactions on Smart Grid*, Vol. 5, No. 2, pp. 1088-1097.

